Chinese-German J Clin Oncol December 2014, Vol. 13, No. 12, P563–P566
DOI 10.1007/s10330-314-0021-9

Phantom-based evaluations of two binning algorithms for four-dimensional CT reconstruction in lung cancer radiation therapy

Fuli Zhang, Huayong Jiang, Weidong Xu, Yadi Wang (✉), Qingzhi Liu, Na Lu, Diandian Chen, Bo Yao

Department of Radiation Oncology, The Military General Hospital of Beijing PLA, Beijing 100700, China

Received: 3 November 2014 / Revised: 17 November 2014 / Accepted: 5 December 2014
© Huazhong University of Science and Technology 2014

Abstract *Objective:* The purpose of this study was to evaluate the performance of the phase-binning algorithm and amplitude-binning algorithm for four-dimensional computed tomography (4DCT) reconstruction in lung cancer radiation therapy. *Methods:* Quasar phantom data were used for evaluation. A phantom of known geometry was mounted on a four-dimensional (4D) motion platform programmed with twelve respiratory waves (twelve lung patients trajectories) and scanned with a Philips Brilliance Big bore 16-slice CT simulator. The 4DCT images were reconstructed using both phase- and amplitude-binning algorithms. Internal target volumes (ITVs) of the phase- and amplitude-binned image sets were compared by evaluation of shape and volume distortions. *Results:* The phantom experiments illustrated that, as expected, maximum inhalation occurred at the 0% amplitude and maximum exhalation occurred at the 50% amplitude of the amplitude-binned 4DCT image sets. The amplitude-binned algorithm rendered smaller ITV than the phase-binning algorithm. *Conclusion:* The amplitude-binning algorithm for 4DCT reconstruction may have a potential advantage in reducing the margin and protecting normal lung tissue from unnecessary irradiation.

Key words four-dimensional computed tomography (4DCT); phase-binning algorithm; amplitude-binning algorithm; lung cancer

Respiratory motion is a significant source of temporal and spatial uncertainty in radiotherapy treatment and can result in planning and radiation delivery errors [1–6]. Motion management techniques such as breath-hold and compression methods are useful in some cases but often uncomfortable, impractical, or impossible for patients. As such, the acquisition and use of four-dimensional computed tomography (4DCT) to measure anatomical motion during quiet respiration is a popular clinical technique in radiation therapy [7].

Early 4DCT reconstruction techniques used phase-binning algorithms for sorting 4D projection data into (typically 10) phases, forming datasets intended to represent a complete breathing cycle [8–15]. In this method, the phase-specific CT image sets were reconstructed by correlating projection data with an external respiratory surrogate during acquisition (usually a tracked marker block or pneumatic belt placed on the patient’s abdomen) and separating projection data acquired during different breathing cycles into phase-angle bins, defined as specific fractions in time between sequential occurrences of a reference breathing phase, such as peak inhalation, and often described as angles in degrees or radians. While phase binning based 4DCT was a logical way of describing the breathing cycle, this binning technique was shown to be prone to image distortions caused by breathing amplitude irregularities during data acquisition. An alternative binning method based on respiratory amplitude has been proposed in hopes of reducing motion artifacts caused by irregular breathing patterns [10–14].

As the terminology insinuates, amplitude-binning technique sorts 4DCT projection data into amplitude-specific datasets according to the corresponding amplitudes of subsequent breathing cycles. Rietzel *et al.* [11] introduced an amplitude-sorting method in which the positions of 4DCT amplitude-specific datasets were designated by fixed amplitude values selected relative to the respiratory waveform. Other similar works have also been reported [10, 12–14, 16–17]. Those studies have found that amplitude-binning algorithms yield less motion artifacts and provide more accurate 4DCT images than phase-binning algorithms for improved treatment planning and delivery. The amplitude-specific datasets are determined by (1) retrospectively assessing the breathing

Correspondence to: Yadi Wang. Email: wangyadi@hotmail.com

wave for the average amplitude values of maximum inhalation and maximum exhalation, (2) interpolating average amplitudes for other eight intermediate amplitudes, and (3) then grouping together projection data with the same respiratory amplitude level from each cycle in the appropriate amplitude-specific bin for reconstruction, in which 0% amplitude represents average maximum inhalation and 50% amplitude average maximum exhalation. In this manner, the reconstructed amplitude-specific images should be less susceptible to motion artifacts caused by fluctuations in respiratory amplitude.

In this paper, we compared the two binning algorithms for retrospective 4DCT image reconstruction via phantom-based imaging studies.

Materials and methods

Data acquisition and motion tracking

In this study, all phantom image data were acquired with a Philips Big Bore 16-slice CT simulator (Philips Healthcare, Cleveland, OH) using retrospective helical 4DCT reconstruction software based on Quasar respiratory motion phantom (Modus medical devices inc., USA) as shown in Fig. 1. An sphere with a diameter of 3 cm was inserted into the phantom to simulate a tumor.

The reconstruction software allowed use of both amplitude and phase binning for on-line image reconstruction. All data for the phantom study were acquired using a 4D retrospective gating protocol (120 kVp, 300 mAs/slice, collimation 16 mm × 1.5 mm, pitch 0.15, rotation time 0.5 s, FOV 500 mm, ultrafast recon kernel, 3 mm slice thickness, 3 mm increment, and standard filter). The 4D phantom was programmed with twelve different motion patterns: all twelve trajectories modeled from real patient respiratory motion. The twelve real patient respiratory waves programmed into the motion phantom were derived from breathing wave data files obtained with the Philips bellows device. The data files were collected during the clinical 4DCT of twelve lung cancer patients. A typical patient respiratory wave was shown in Fig. 2.

Phase-binning algorithm for 4DCT image reconstruction

In the phase-binning process, respiratory tags were placed in a semiautomatic fashion at the local maxima of each breathing cycle in the respiratory waveform to determine the 0% phase point (peak inhalation). Projection data were then sorted into 10 phase-angle bins, subdivided in 10% temporal increments of the breathing period. Ten 4DCT image sets representing these phase angles were reconstructed from the binned data. The CT image set representing 0% phase angle reconstruction was the maximum inhalation data set. Because the shape of a patient breathing wave was not typically symmetrical, the maximum exhalation data set most often occurred in the 40%, 50%, or 60% phase-angle reconstructions. A typical series of CT images by phase-binning algorithm was shown in Fig. 3.

Amplitude-binning algorithm for 4DCT image reconstruction

In the amplitude-binning process, the peaks (maximum inhalation) were detected for each cycle in a semiautomatic manner, like the phase-binning method. Additionally, the valleys (maximum exhalation) were also detected. The average peak and valley amplitudes were computed to determine the amplitude value of the 0% amplitude point and 50% amplitude point. Average amplitudes for intermediate data sets were interpolated to construct the rest eight amplitude-specific bins. As such, in amplitude-binning algorithms, the 0% amplitude represented the average maximum inhalation, and the 50% amplitude represented the average maximum exhalation, which may deviate slightly since data were acquired over 0.5 s of gantry rotation, and thus was not instantaneous. A typical series of CT images by amplitude-binning algorithm was shown in Fig. 4.

Tumor segmentation and data analysis

In order to compare the image quality of both 4DCT reconstruction algorithms, we used the autosegmentation tool provided by Mimvista Version 6.0.2 (MIMVista corp, Cleveland, Ohio) to measure the sphere volume in the image data set. The same threshold level was used for all the cases to ensure consistency. For each slice, a region of interest (ROI) enclosing the sphere was defined, and then, the sphere was automatically contoured. Then, the internal target volume (ITV_{10}) was acquired by uniting the 0%–90% series of CT images. Contours were also retrospectively reviewed (but not modified) to ensure contour accuracy. The reference sphere structure from the 3D stationary scan was also extracted in the same way.

One additional metrics were defined to assess the volumetric distortions of the imaged sphere. First, the ratio of

$$\text{Volume ratio} = V_{ITV}\frac{V_{ITV}}{V_{standard}} \times 100\% \quad (1)$$

an ITV_{10} to the actual sphere volume was defined as the volumetric ratio (1).

Statistical analysis

A paired *t*-test was performed to evaluate significant differences between phase- and amplitude-binned image sets. Statistical significance was set at $P < 0.05$.

Results

The phantom experiments illustrated that, as expected, the 0% amplitude-specific images reflected average maximum inhalation. Amplitude gated images exhibited

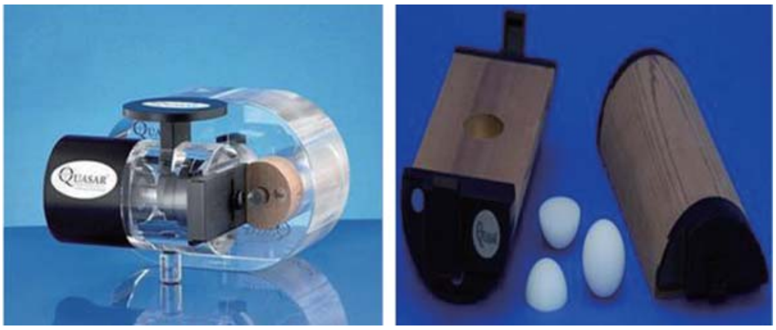

Fig. 1 Modus respiratory motion phantom and tumor inserts

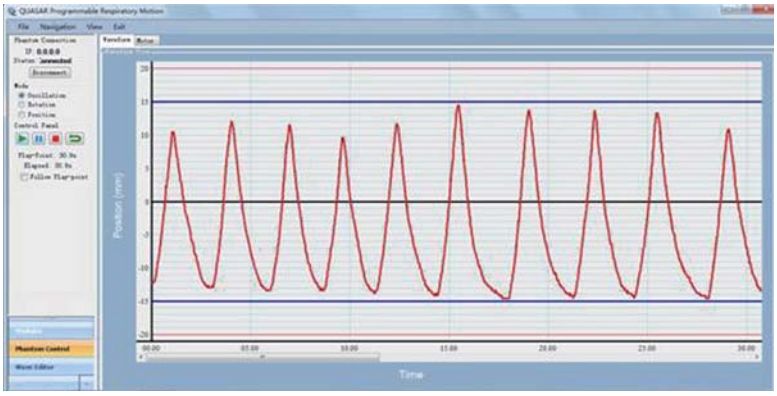

Fig. 2 A typical patient respiratory wave

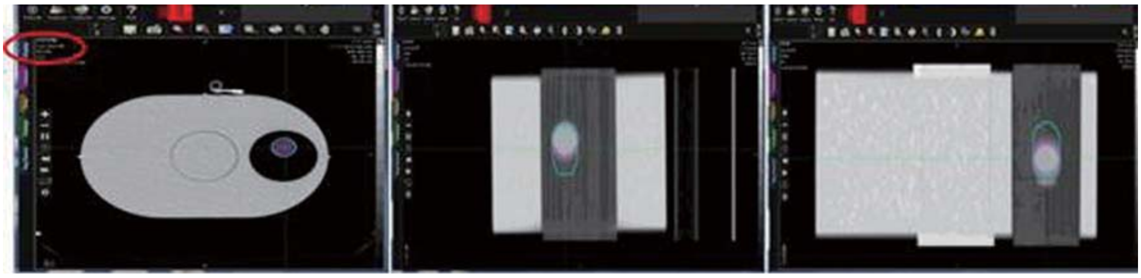

Fig. 3 A typical series of CT images in transverse, sagittal, coronal view by phase-binning algorithm

Fig. 4 A typical series of CT images in transverse, sagittal, coronal view by amplitude-binning algorithm

maximum exhalation at the 50% amplitude-specific images. The volumetric ratios varied with different respiratory waves and phase-binning algorithm acquired a larger ratio than amplitude-binning algorithm (1.60 ± 0.47 vs 1.55 ± 0.96, $P = 0.536$), as shown in Table 1.

Discussion

As explained in the methodology, the amplitude-binning algorithm generates the 0% and 50% amplitude-specific image sets using the average peak and average valley

Table 1 Comparison of phase-ITV_{10} and amplitude-ITV_{10}

Patient No.	Phase-ITV_{10} (cm^3)	Amplitude-ITV_{10} (cm^3)
1	14.82	14.51
2	29.55	25.94
3	20.33	14.65
4	16.32	14.56
5	18.79	22.38
6	11.44	11.20
7	20.93	28.08
8	22.52	18.65
9	29.11	30.06
10	32.28	27.02
11	27.42	26.05
12	27.50	29.57
$\overline{x}$	22.58	21.89
s	6.60	6.81
P	0.536	

Note: Phase-ITV_{10} meaning the volume by phase-binning algorithm while Amplitude-ITV_{10} meaning the volume by amplitude-binning algorithm

amplitude levels (respectively) of the respiratory wave. Thus, the full range of motion may not be characterized using this binning algorithm. This probably explains why seven total phantom studies resulted in smaller ITVs on amplitude-binned image sets compared to phase-binned image sets. Amplitude-based binning algorithms may offer an important advantage for clinical workflow. Most institutions employing gated treatment set the daily gating window based on the amplitude of the patient's respiratory wave. Since gated treatments are most often triggered using amplitude-based gating, phase-based 4DCT reconstruction is inconsistent with common treatment practice. From this aspect, an amplitude-binning algorithm is more suitable for the treatment plan delivery.

Due to smaller patient number in this study, it is difficult to derive a statistically significant result for the influence of different binning algorithms on the delineation of target volume and dose calculation accuracy that will be studied in our further study.

Conclusions

This paper provides an experimental evaluation of the two binning algorithms for 4DCT imaging. Overall, the amplitude-binning algorithm for 4DCT reconstruction may have a potential advantage in reducing the margin and protecting normal lung tissue from unnecessary irradiation compared to the phase-binning algorithm.

Conflicts of interest

The authors indicated no potential conflicts of interest.

References

1. Low DA, Nystrom M, Kalinin E, *et al.* A method for the reconstruction of four-dimensional synchronized CT scans acquired during free breathing. Med Phys, 2003, 30: 1254–1263.
2. Ford EC, Mageras GS, Yorke E, *et al*. Respiration-correlated spiral CT: a method of measuring respiratory-induced anatomic motion for radiation treatment planning. Med Phys, 2003, 30: 88–97.
3. Pan T, Lee TY, Rietzel E, *et al.* 4D-CT imaging of a volume influenced by respiratory motion on multi-slice CT. Med Phys, 2004, 31: 333–340.
4. Rietzel E, Chen GT, Choi NC, *et al.* Four-dimensional image-based treatment planning: Target volume segmentation and dose calculation in the presence of respiratory motion. Int J Radiat Oncol Biol Phys, 2005, 61: 1535–1550.
5. Rietzel E, Pan T, Chen GT. Four-dimensional computed tomography: image formation and clinical protocol. Med Phys, 2005, 32: 874–889.
6. Zhang FL, Zheng MM, Zhang JB, *et al*. An anthropomorphic phantom study of effect of lung tumor size and location on dosimetric parameters. Chinese-German J Clin Oncol, 2010, 9: 133–136.
7. Li H, Noel C, Garcia-Ramirez J, *et al*. Clinical evaluations of an amplitude-based binning algorithm for 4DCT reconstruction in radiation therapy. Med Phys, 2012, 39: 922–932.
8. Guckenberger M, Wilbert J, Krieger T, *et al*. Mid-ventilation concept for mobile pulmonary tumors: internal tumor trajectory versus selective reconstruction of four-dimensional computed tomography frames based on external breathing motion. Int J Radiat Oncol Biol Phys, 2009, 74: 602–609.
9. Park K, Huang L, Gagne H, *et al*. Do maximum intensity projection images truly capture tumor motion? Int J Radiat Oncol Biol Phys, 2009, 73: 618–625.
10. Santoro JP, Yorke E, Goodman KA, *et al*. From phase-based to displacement-based gating: a software tool to facilitate respiration-gated radiation treatment. J Appl Clin Med Phys, 2009,10: 2982.
11. Rietzel E, Chen GT. Improving retrospective sorting of 4D computed tomography data. Med Phys, 2006, 33: 377–379.
12. Wink N, Panknin C, Solberg TD. Phase versus amplitude sorting of 4D-CT data. J Appl Clin Med Phys, 2006, 7: 77–85.
13. Abdelnour AF, Nehmeh SA, Pan T, *et al*. Phase and amplitude binning for 4D-CT imaging. Phys Med Biol, 2007, 52: 3515–3529.
14. Olsen JR, Lu W, Hubenschmidt JP, *et al.* Effect of novel amplitude/phase binning algorithm on commercial four-dimensional computed tomography quality. Int J Radiat Oncol Biol Phys, 2008, 70: 243–252.
15. Rietzel E, Liu AK, Chen GT, *et al*. Maximum-intensity volumes for fast contouring of lung tumors including respiratory motion in 4DCT planning. Int J Radiat Oncol Biol Phys, 2008, 71: 1245–1252.
16. Lu W, Parikh PJ, Hubenschmidt JP, *et al*. A comparison between amplitude sorting and phase-angle sorting using external respiratory measurement for 4D CT. Med Phys, 2006, 33: 2964–2974.
17. Rietzel E, Liu AK, Doppke KP, *et al.* Design of 4D treatment planning target volumes. Int J Radiat Oncol Biol Phys, 2006, 66: 287–295.

DOI 10.1007/s10330-314-0021-9
Cite this article as: Zhang FL, Jiang HY, Xu WD, *et al*. Phantom-based evaluations of two binning algorithms for four-dimensional CT reconstruction in lung cancer radiation therapy. Chinese-German J Clin Oncol, 2014, 13: 563–566.